

# Avoiding unstable regions in the design space of EUV mirror systems comprising high-order aspheric surfaces

Oana Marinescu\*, Florian Bociort, Joseph Braat

Optics Research Group, Delft University of Technology  
Lorentzweg 1, NL - 2628 CJ Delft, The Netherlands

## ABSTRACT

When Extreme Ultraviolet mirror systems having several high-order aspheric surfaces are optimized, the configurations often enter into highly unstable regions of the parameter space. Small changes of system parameters lead then to large changes in ray paths, and therefore optimization algorithms crash because certain assumptions upon which they are based become invalid. We describe a technique that keeps the configuration away from the unstable regions. The central component of our technique is a finite-aberration quantity, the so-called quasi-invariant, which has been originally introduced by H. A. Buchdahl. The quasi-invariant is computed for several rays in the system, and its average change per surface is determined for all surfaces. Small values of these average changes indicate stability. The stabilization technique consists of two steps: First, we obtain a stable initial configuration for subsequent optimization by choosing the system parameters such that the quasi-invariant change per surface is minimal. Then, if the average changes per surfaces of the quasi-invariant remain small during optimization, the configuration is kept in the safe region of the parameter space. This technique is applicable for arbitrary rotationally symmetric optical systems. Examples from the design of aspheric mirror systems for EUV lithography will be given.

**Keywords:** mirror systems, aspheres, EUV lithography, optimization, relaxation

## 1. INTRODUCTION

In optical system design, it is often important to decrease the sensitivity of the imaging quality of the design when system parameters are slightly changed. For instance, in "relaxed" designs, in which the permissible tolerances for a given deterioration in image quality are not very restrictive, high-order aberrations are kept at low levels<sup>1</sup>. In this case, if third-order aberration analysis is used, not only the total values of the (relevant) Seidel coefficients must be sufficiently low, but the individual contributions of the various surfaces to these coefficients must be kept within limits as well<sup>2</sup>. Surfaces where individual surface contributions to the Seidel coefficients are too large tend to generate high-order aberrations and the total system will suffer from "strain" (the opposite of "relaxation") even when the resulting imaging quality is satisfactory.

Our special interests in this paper are rotationally symmetric systems having many high-order aspheric surfaces, such as the Extreme Ultraviolet (EUV) lithographic objectives. When such systems are optimized with the aspheric coefficients as variables, the configurations often evolve toward shapes in which the "strain" is so extreme that optimization itself becomes difficult. When small changes to system parameters lead to large changes in the ray paths, optimization algorithms tend to become unstable and to terminate abnormally.

We present a strategy to avoid such unstable regions in the parameter space of the system. After introducing in Sec.2 some paraxial prerequisites, we will introduce in Sec.3 a finite-aberration quantity, the so-called quasi-invariant. Our quasi-invariant is almost identical with the one originally introduced by H. A. Buchdahl<sup>3</sup> for a very different purpose,

---

\* [o.marinescu@tw.tudelft.nl](mailto:o.marinescu@tw.tudelft.nl) phone +31 15 2788109; fax +31 15 278 8105

namely to compute high-order aberration coefficients. Whereas the Seidel aberrations contain only the 4th order aspheric surface coefficient, the quasi-invariant contains the aspheric coefficients for all orders. In Sec. 4 we show how the quasi-invariant can be used to stabilize the optimization. Basically, we generalize for finite rays the idea mentioned above of limiting the acceptable magnitude of the contributions of individual surfaces to the aberrations of the system. In principle, the same basic idea could also be implemented by using the so-called Aldis theorem<sup>4</sup>, but in our opinion the use of the quasi-invariant is simpler and more straightforward.

## 2. PARAXIAL APPROXIMATION

Consider a rotationally symmetric optical system. We denote the object plane by O, the paraxial image plane by I and the stop plane by S. We define an arbitrary ray through the system by its normalized coordinates in the object plane  $(\tau_x, \tau_y)$ -the field coordinates and in the stop plane  $(\sigma_x, \sigma_y)$ -the aperture coordinates. Thus, if the stop radius is  $r_s$  and the maximal object height is  $r_o$ , then the Cartesian coordinates are related to the normalized coordinates at the stop plane by

$$x_s = r_s \sigma_x, \quad y_s = r_s \sigma_y \quad (1)$$

and at the object plane by

$$x_o = r_o \tau_x, \quad y_o = r_o \tau_y \quad (2)$$

At each surface, the position and direction of a ray passing through the system are fully determined by the  $x$  and  $y$  coordinates of its point of intersection with the surface and by the optical direction cosines  $\xi$  and  $\eta$ , corresponding to  $x$  and  $y$ . (The optical direction cosines are the direction cosines multiplied by the refractive index.)

$$\begin{aligned} \xi &= nL \\ \eta &= nM \end{aligned} \quad (3)$$

It can be shown<sup>3, 5, 6</sup> that in the paraxial approximation  $x$ ,  $y$ ,  $\xi$  and  $\eta$  are for all surfaces of the system given by linear combinations of the aperture and field coordinates. The coefficients are then height and slope of the paraxially traced marginal and chief rays at that surface. If we denote paraxial coordinates by a tilde, we have

$$\begin{aligned} \tilde{x} &= \bar{h} \tau_x + h \sigma_x, & \tilde{\xi} &= n\bar{u} \tau_x + nu \sigma_x \\ \tilde{y} &= \bar{h} \tau_y + h \sigma_y, & \tilde{\eta} &= n\bar{u} \tau_y + nu \sigma_y \end{aligned} \quad (4)$$

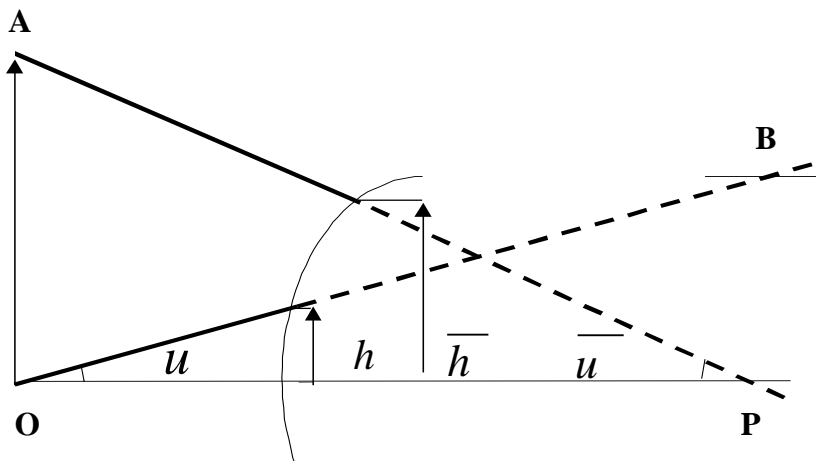


**Figure 1.** Paraxial heights and slopes of the marginal ray OB and chief ray AP at an arbitrary surface.

Here, the paraxial marginal and chief ray heights are denoted  $h$  and  $\bar{h}$ , the corresponding marginal and chief ray slopes are denoted  $u$  and  $\bar{u}$  and the refractive index is denoted by  $n$  (See Figure 1). In the case of mirror systems, which we study here, the refractive index  $n$  equals  $\pm 1$ , the sign changing after each reflection.

We will also use the fact that  $h$ ,  $\bar{h}$ ,  $u$ ,  $\bar{u}$  are not independent. In fact, the quantity  $H$  defined by

$$H = n\bar{h}u - nh\bar{u} \quad (5)$$

(the Lagrange invariant) retains the same value throughout the system. (See e.g. 5). It plays an essential role in Buchdahl's deductions.

In Eq. (4),  $n$ ,  $u$ ,  $\bar{u}$ ,  $\xi$  and  $\eta$  are quantities prior to reflection or refraction. Of course, similar relations exist for the corresponding quantities after reflection or refraction.

### 3. QUASI-INVARIANTS

For an arbitrary finite ray, consider the two components of the transverse aberration vector of the ray. As usual, these components are defined at the paraxial image plane by

$$\Xi_x = x_I - \tilde{x}_I, \quad \Xi_y = y_I - \tilde{y}_I \quad (6)$$

Consider first Eqs. (4), which hold for the paraxial approximations of the ray parameters. We start by seeking certain quantities, which can be related to the given ray such that relations similar to Eqs. (4) hold exactly for them. More precisely, we look for eight quantities  $\hat{x}$ ,  $\hat{y}$ ,  $\hat{\xi}$ ,  $\hat{\eta}$ ,  $\hat{\sigma}_x$ ,  $\hat{\sigma}_y$ ,  $\hat{\tau}_x$ ,  $\hat{\tau}_y$  such that at every surface of the system we have

$$\begin{aligned} \hat{x} &= \bar{h} \hat{\tau}_x + h \hat{\sigma}_x, & \hat{\xi} &= n\bar{u} \hat{\tau}_x + nu \hat{\sigma}_x \\ \hat{y} &= \bar{h} \hat{\tau}_y + h \hat{\sigma}_y, & \hat{\eta} &= n\bar{u} \hat{\tau}_y + nu \hat{\sigma}_y \end{aligned} \quad (7)$$

The first requirement for determining the new quantities is that in the paraxial approximation Eqs. (7) reduce to Eqs. (4). Thus, the paraxial approximations for  $\hat{\sigma}_x$ ,  $\hat{\sigma}_y$ ,  $\hat{\tau}_x$ ,  $\hat{\tau}_y$  must be the quantities  $\sigma_x$ ,  $\sigma_y$ ,  $\tau_x$ ,  $\tau_y$ , which by definition ((1) and (2)) are surface-independent. Following Buchdahl, any quantity which reduces to such an invariant in the paraxial limit will be called a quasi-invariant. Clearly,  $\hat{\sigma}_x$ ,  $\hat{\sigma}_y$ ,  $\hat{\tau}_x$ ,  $\hat{\tau}_y$  are such quantities.

The basic idea is now to relate the aberrations produced by each surface to the changes of the quasi-invariants at that surface. Therefore, since the normalized coordinates are defined at the object and stop planes, we require that the quasi-invariants associated to the field and aperture coordinates are free of aberrations at the object and stop planes, respectively, i.e. that they reduce to the corresponding ray coordinates,

$$\hat{\tau}_{xO} = \tau_x, \quad \hat{\tau}_{yO} = \tau_y \quad (8)$$

and

$$\hat{\sigma}_{xS} = \sigma_x, \quad \hat{\sigma}_{yS} = \sigma_y \quad (9)$$

Since at the object plane we have  $\bar{h} = r_O$  and  $h = 0$  and at the stop plane we have  $h = r_S$  and  $\bar{h} = 0$ , it follows by comparing Eq. (7) with Eqs. (1) and (2) that at these two planes we have

$$\hat{x} = x, \quad \hat{y} = y \quad (10)$$

We now require that Eq. (10) must be valid at each plane surface.

The components  $\Xi_x$  and  $\Xi_y$  of the transverse aberration can be expressed through the quasi-invariants. By denoting the maximal paraxial image height by  $r_I$ , it follows from Eq. (6) that

$$\Xi_x = x_I - \tilde{x}_I = r_I (\hat{\tau}_{xI} - \tau_x) \quad (11)$$

A similar relation is valid for the y-component. Let us however consider for the moment only the x-component. Obviously, the total change of  $\hat{\tau}_x$  from the object to the image plane can be written as sum of all individual changes in the system

$$\hat{\tau}_{xI} - \tau_x = \hat{\tau}_{xI} - \tau_{xO} = \sum \Delta \hat{\tau}_x \quad (12)$$

For determining the expressions of the quasi-invariants, consider Eq. (7) as systems of linear equations with unknowns  $\hat{\sigma}_x$ ,  $\hat{\sigma}_y$ ,  $\hat{\tau}_x$ ,  $\hat{\tau}_y$ . It follows from Eqs. (7) and (5) that at each surface of the system we have

$$\hat{\tau}_x = \frac{1}{H} (nu\hat{x} - h\hat{\xi}) \quad (13)$$

and

$$\hat{\sigma}_x = -\frac{1}{H} (n\bar{u}\hat{x} - \bar{h}\hat{\xi}) \quad (14)$$

Let us now determine the precise form of  $\hat{x}$ ,  $\hat{y}$ ,  $\hat{\xi}$  and  $\hat{\eta}$ . The usual assumption in aberration theory is that transfer through a homogeneous medium does not contribute to the aberrations. Therefore, we simply require that the change of  $\hat{\tau}_x$  vanishes at transfer through a homogeneous medium.

Consider first the case of the transfer between two planes separated by the distance  $z$ . It can be easily verified that the transfer contributions vanish for

$$\hat{\xi} = \frac{n\xi}{\zeta}, \quad \hat{\eta} = \frac{n\eta}{\zeta} \quad (15)$$

where  $\zeta$  is the optical direction cosine with respect to the z-axis,

$$\zeta = \sqrt{n^2 - \xi^2 - \eta^2} \quad (16)$$

Note that  $\zeta = nN$ , where  $N$  is the direction cosine along the z-axis. In the case of mirror systems  $n$  and  $N$  have the same sign (that changes after each reflection), so  $\zeta$  will always be positive.

In fact, at transfer,  $n$ ,  $u$ ,  $\xi$  and  $\zeta$  remain unchanged. Thus, we have

$$\Delta \hat{x} = \Delta x = \frac{\xi}{\zeta} z, \quad \Delta h = uz \quad (17)$$

and therefore

$$\Delta \hat{\tau}_x = \frac{1}{H} (nu\Delta x - \frac{n\xi}{\zeta} \Delta h) = 0 \quad (18)$$

Consider now the case of transfer between two curved mirror or lens surfaces. At every surface we consider the plane tangent to the surface at its vertex (the polar tangent plane). Obviously, Eq. (18) also holds if instead of  $x$  we consider the quantity  $\hat{x}$  defined as the x-coordinate of the intersection point of the transferred ray (or its prolongation) with the corresponding polar tangent plane. Thus, the quantities  $\hat{x}$  and  $\hat{y}$  in Eq. (7) must be the polar-tangent-plane coordinates of the given ray. (See Figure 2). Thus, the quasi-invariant  $\hat{\tau}_x$  has non-zero changes  $\Delta \hat{\tau}_x$  at the individual surfaces and in Eq. (12) the sum must be taken over all surface. Note that for each ray-surface intersection point, we have two values for  $\hat{x}$  (and  $\hat{y}$ ): one before and one after reflection or refraction. Having established the form of the quantities appearing in Eq. (7), note that relations similar to (13) and (14) can be written for  $\hat{\tau}_y$  and  $\hat{\sigma}_y$

$$\hat{t}_y = \frac{1}{H}(nu\hat{y} - h\hat{\eta})$$

$$\hat{\sigma}_y = -\frac{1}{H}(n\bar{u}\hat{y} - h\bar{\eta})$$
(19)

If at the paraxial image plane we write  $H = r_1 n_1 u_1$ , it follows from Eqs. (10) and (11) that

$$\Xi_x = \frac{1}{n_1 u_1} \Sigma \Delta(H \hat{t}_x)$$
(20)

a similar relation being valid for  $\Xi_y$ . Equation (20) gives the decomposition of the transverse aberration of an arbitrary ray in contributions from reflection or refraction at each surface of the system. Since the two components of the  $\hat{t}$  quasi-invariant are related to the transverse aberration, this quasi-invariant plays a more important role than  $\hat{\sigma}$ .

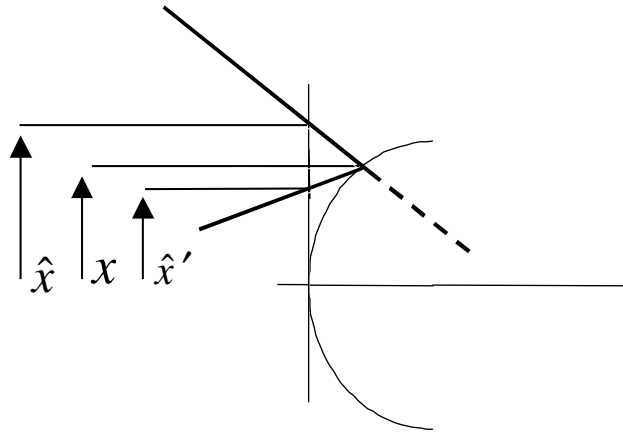


**Figure 2.** The quantities  $\hat{x}$  before and  $\hat{x}'$  after reflection of a ray at a mirror surface. The quantities  $\hat{y}$  and  $\hat{y}'$  are defined similarly. These four quantities are necessary for computing  $\Delta \hat{t}_x$  and  $\Delta \hat{t}_y$ .

These quasi-invariants can also be used for deriving analytic expressions for Seidel and higher-order aberrations coefficients<sup>6</sup>. In a power series expansion with respect to the aperture and field coordinates the third-order terms of  $\Delta(H \hat{t}_x)$  and  $\Delta(H \hat{t}_y)$  are the aberration coefficients.

#### 4. STABILIZING THE OPTIMIZATION

Extreme Ultraviolet mirror-designs typically have 4, 6 or 8 high-order aspherical surfaces. A standard aspherical surface with rotational symmetry about the z-axis can be represented as:

$$z = \frac{c(x^2 + y^2)}{1 + \sqrt{1 - (1+k)c^2(x^2 + y^2)}} + \sum_{n=2}^{n_0} a_{2n}(x^2 + y^2)^{2n}$$
(21)

where  $c$  is the curvature at the vertex of the surface,  $k$  is the conic constant and  $a_{2n}$  are polynomial coefficients ( $n = 2, \dots, n_0$ ). Such systems often enter into highly unstable regions of the parameter space during optimization. In this section we show how to avoid this problem based on the idea that there is a correlation between the change in the quasi-invariant and the system sensitivity. According to Eq. (20), large aberrations at a surface lead to large increase at the  $\hat{t}$  quasi-invariant at that surface (At the time of this writing constraints on  $\Delta \hat{t}$  seem to be sufficient for achieving the envisaged

goal. If necessary, the path of real rays can be brought even closer to the paraxial ones if constraints are imposed on  $\Delta\hat{\sigma}$  as well).

Inspired by the Seidel analogy mentioned in the introduction the algorithm presented below (See also Figure 3) keeps the aberrations per surface at an acceptable low level during optimization.

For computing  $\hat{x}$  and  $\hat{y}$ , the program introduces automatically two dummy surfaces at each surface (one before the surface and one after it). Once there, they will behave as tangent planes to that surface (See Figure 2). The quasi-invariant before and after the surface is then computed from ray-tracing data at the surfaces (See Eq. (13)).

At each surface, for each field point, the quasi-invariant is calculated for  $m$  rays. (At present we use four rays per field: chief ray, upper and lower marginal rays and a skew ray.<sup>7</sup>) The average change of the quasi-invariant at the surface,  $\overline{\Delta\tau}$ , is then:

$$\overline{\Delta\tau} = \sqrt{\frac{\sum_{i=1}^m \Delta\hat{\tau}_{x,i}^2 + \Delta\hat{\tau}_{y,i}^2}{m}} \quad (22)$$

A design, which would normally fall into unstable regions of the merit function space during local optimization, is stabilized in two stages. In the first stage, the variables on each surface are arranged so that the design is stable. At this stage, by minimizing the change of the quasi-invariant at each surface, optimization is used surface by surface to generate surface shapes that lead to a stable ray path. The process is performed for all surfaces. When going to the next surface, the program will automatically freeze the variables already used and introduce new ones for that surface.

In the second stage, the imaging quality is again optimized surface by surface with the additional constraint  $\overline{\Delta\tau} < \lambda$ , where  $\lambda$  is chosen on the bases of experience. If the maximal change per surface of the quasi-invariant remains small during optimization the configuration is kept in the safe region of the parameter space. When the stabilization attempt is not successful, the parameter  $\lambda$  is changed and the process is repeated. At the end of the process all dummy surfaces will be automatically removed. Finally, the quasi-invariant constraint is removed and conventional optimization is performed again. The solution obtained by quasi-invariant (QI) optimization is usually a local minimum in the merit function space that is different from the one obtained by optimizing the initial configuration without quasi-invariant.

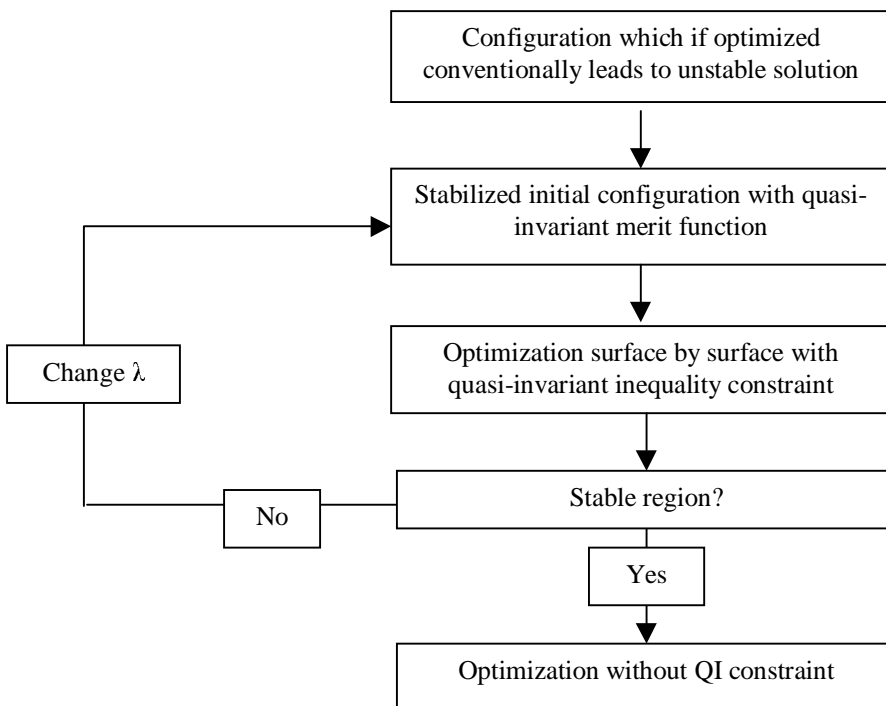


**Figure 3.** Flow chart for QI optimization.

As an example we present below several results obtained for six-mirror EUV objectives. Figure 4 shows an optimized six-mirror system. According to the classification scheme discussed in Ref. 8 the system belongs to class 37+. All six curvatures and the aspheric coefficients of 4<sup>th</sup> and 6<sup>th</sup> order on each surface are used as variables. The image plane is placed at the paraxial position and the first distance is solved to keep the constant magnification of 0.25. To the default merit function of Code V the quasi-invariant is added as a constraint. The system is kept quasi-telecentric in the object space and telecentric in the image space, i.e. the upper marginal ray in the object space and the chief ray in the image space are parallel to the optical axis. Distortion is also controlled.

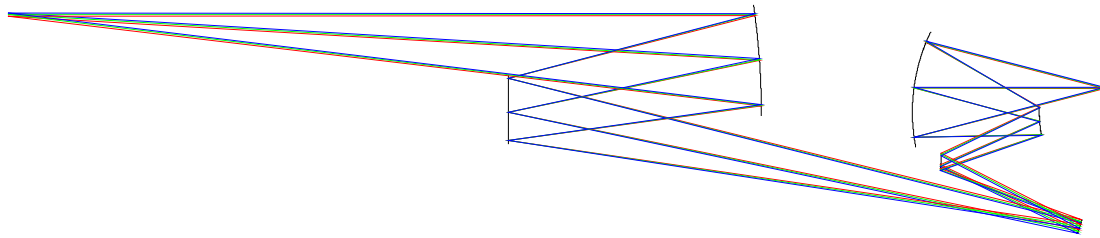


**Figure 4.** Six-mirror system in class 37+ stabilized with the quasi-invariant method, with object heights between 114 and 118 mm, a numerical aperture of 0.24 and a magnification of 0.25.

The histograms in Figure 5 present the evolution of the variables during conventional and QI optimizations. Figure 5a shows how the curvatures behave and Figure 5b shows the behavior of the 6<sup>th</sup> order aspheres (See Eq. (21)) at each surface. Note that the quasi-invariant results presented here correspond to the stage immediately before the final conventional optimization. We observe that while the heights of the bars in Figure 5a are roughly the same, Figure 5b presents a large variation in the values and the orientation of the bars. The difference between the conventional and qi optimization is due to the aspheric coefficients. For instance, the 6<sup>th</sup> order aspheric coefficient at the fifth surface is much larger than in the qi result. In the conventional result, we have observed that even a small change in one of the parameters can cause large changes in the rays path and thus in the performance of the system. In our experience the aspheres are more likely to push the systems in regions of instability than the curvatures.

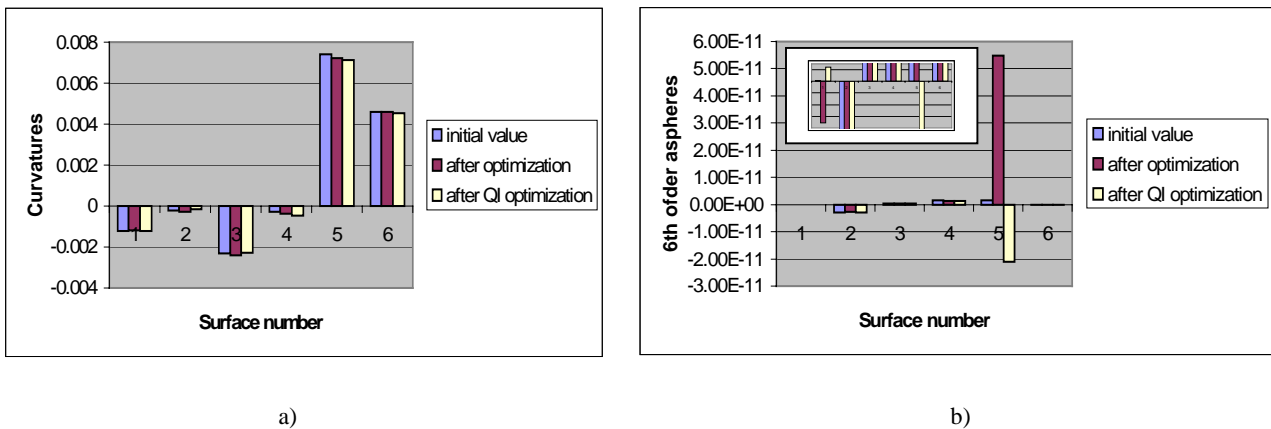


**Figure 5.** Histogram indicating the evolution of the variables during conventional and qi optimization. a) curvatures; b) the 6<sup>th</sup> order aspheres at each surface. In the insert the bars corresponding to the surfaces are enlarged.

The sensitivity to changes in the parameters has been monitored for systems with different order of aspheres. In the case of the 4<sup>th</sup> order aspheres that induce instability in the system we have analyzed the behavior of the Seidel aberrations as well. Even if the Seidel sums for the unstable system are lower than for the QI-optimized system, the latter optimization leads to smaller values for the aberrations per surface and succeeds in keeping the system in the stable region of the merit

function space. For virtually all cases we have studied, the QI-optimization was able to push the system in the basin of attraction of a more stable configuration.

## CONCLUSIONS

In this paper we have presented a new method to stabilize the optimization process of EUV mirror systems having high-order aspheres. The optimization with the quasi-invariant constraint has been applied to several projection systems and after the system was stabilized, subsequent conventional optimization was successful in most cases. An example of an EUV mirror system that has been placed in the stable region of the parameter space has been discussed in more detail. In this paper the emphasis was on mirror systems. However, the same technique could be useful for different applications as well.

## ACKNOWLEDGEMENTS

The first author would like to gratefully acknowledge the financial support of ASML.

## REFERENCES

1. D. Shafer, "Optical design and the relaxation response", *Proc. SPIE*, **0766**, 2-9, 1987
2. M. Berek, *Grundlagen der praktischen Optik*, Walter de Gruyter, Leipzig, 1930
3. H.A. Buchdahl, *Optical Aberration Coefficients*, Dover, New York, 1968
4. W. T. Welford, *Aberrations of Optical Systems*, Adam Hilger, Bristol, 1986
5. H.H. Hopkins, "The nature of paraxial approximation", *J. Mod. Opt.*, **38**, 427-472, 1991
6. F. Bociort, "Computer algebra derivation of high-order optical aberration coefficients", Riaca Technical Report no 7, Amsterdam, 1995, also available at <http://www.optica.tn.tudelft.nl/users/bociort/riaca.pdf>
7. In the CodeV manual these rays are called R<sub>1</sub>, R<sub>2</sub>, R<sub>3</sub>, R<sub>4</sub>. CodeV 9.40, Manual, Optical Research Associates, Pasadena, 2004
8. M. Bal, F. Bociort, J.J.M.Braat, "Analysis, search, and classification for reflective ring-field projection optics", *Appl. Opt.* **42** (13), 2301-2311, 2003